Vacuum 219 (2024) 112657

Contents lists available at ScienceDirect

Vacuum

journal homepage: www.elsevier.com/locate/vacuum

RF magnetron sputtered Nb–V–N composite coatings for high-temperature self-lubricant applications

Moussa Athmani [a,1], FanLin Kong [b,1], Hongbo Ju [b,c,*], Jing Luan [c], Chengke Zhang [b], Bingyang Ma [d], Albano Cavaleiro [c], Filipe Fernandes [c,e,**]

[a] Laboratory of Physics of Thin Films and Applications, University of Mohamed Khider, BP 145 RP, 07000, Biskra, Algeria
[b] School of Materials Science and Engineering, Jiangsu University of Science and Technology, Mengxi Road 2, Zhenjiang, Jiangsu Province, 212003, China
[c] University of Coimbra, CEMMPRE, ARISE, Department of Mechanical Engineering, Rua Luís Reis Santos, 3030-788, Coimbra, Portugal
[d] School of Materials Science, Shanghai Dianji University, Shanghai, 200240, PR China
[e] ISEP, Polytechnic of Porto, Rua Dr. António Bernardino de Almeida, 4249-015 Porto, Portugal

ARTICLE INFO

Handling Editor: Prof. L.G. Hultman

Keywords:
RF magnetron sputtering
Nb–V–N coatings
Mechanical properties
Tribological properties

ABSTRACT

Enhancing the tribological properties of hard ceramic coatings for high temperature applications is one of the hot topics in the solid lubricant field. In this paper, a series of Nb–V–N coatings with different V concentrations were deposited using RF magnetron sputtering system, and the crystalline structure, mechanical and tribological properties were investigated. Results showed that the Nb–V–N coatings regardless of V concentrations exhibited two phase fcc-NbN with V in solid solution and hcp-NbN phase. The hardness and elastic modulus of the coatings were enhanced by adding 5.3 at.% of V. The room temperature tribological properties of the coatings were improved by the addition of V well due to the enhanced mechanical properties and the nature excellent self-lubricant characteristics. The evaluation of main tribophase from the wear track at elevated temperatures from the self-lubricant V_2O_3 at 400 °C to the V_2O_5 at 800 °C, contributed to the stable and excellent anti-frictional properties of the coating with a V concentration of 12.4 at.%. However, the wear rate of the coatings drops gradually with the increase of V concentrations due to the large amount of soft but lubricant tribophases at elevated temperatures.

1. Introduction

Transition metal nitrides, such as NbN, are widely used in the field of tooling due to their excellent mechanical and thermal stability [1]. However, the high friction coefficient and wear rate of these coatings limit their application in industry [2]. In the past decade, V has become one of the hot research elements to develop self-lubricant coatings for high temperature applications, where low friction in the absence of liquid lubrication is required [3,4]. For example, adding V into CrN coating by magnetron sputtering can significantly improve the friction and wear properties of the coating at room temperature, which is caused by the presence of V–O phases on the contact [5]. In the Ti–V–N coatings results showed that the addition of V element can markedly improve the mechanical properties and the friction and wear properties under room temperature and high temperature environment [6]. Moreover, the TiSiN/CrVxN was deposited using the magnetron sputtering system, and the effect of the V on the oxidation resistance and tribological properties were investigated. Results showed that the V ions in the films could diffusion towards to the surface of the film and form the layered V-based oxide phase [7]. NbN coating has excellent mechanical properties, while their tribological properties at room temperature are not ideal [8–10]. Furthermore, previous studies have shown that the high-temperature friction coefficient and wear properties of NbN coating also need to be further improved [11–13]. In this work, the influence of V additions on the properties of a NbN coating was investigated. The crystal structure, mechanical and tribological properties were accessed.

* Corresponding author. School of Materials Science and Engineering, Jiangsu University of Science and Technology, Mengxi Road 2, Zhenjiang, Jiangsu Province, 212003, China.
** Corresponding author. ISEP, Polytechnic of Porto, Rua Dr. António Bernardino de Almeida, 4249-015 Porto, Portugal.
E-mail addresses: hbju@just.edu.cn, hju@uc.pt (H. Ju), fid@isep.ipp.pt (F. Fernandes).
[1] frist co-author.

https://doi.org/10.1016/j.vacuum.2023.112657
Received 8 June 2023; Received in revised form 22 September 2023; Accepted 26 September 2023
Available online 29 September 2023

2. Experiment part

A series of Nb–V–N composite coatings with various V content was synthesized by RF magnetron sputtering system using targets of Nb (99.9%) and V (99%) with a diameter of 75 mm and Ar: N_2(50:1.6) gas mixture. The coatings were deposited silicon wafer with (100) preferential orientation and mirror-finished W18Cr4V high speed steel. All of the substrates were ultrasonically cleaned in alcohol and acetone for 15 min respectively, then hot air dried. The substrates were placed on the substrate holder in the chamber. The detailed deposition parameters are as follows: (1) the base pressure was below 6×10^{-4} Pa, (2) a Nb transition layer having a thickness of about 0.2 μm was deposited on the substrates under pure Ar gas to improve the adhesion of the coatings, (3) Nb (99.9%) and V (99.9%) target power was fixed at 250w, (4) rotate speed of substrate holder was 4 rpm, (5) substrate heating and bias voltage were 100 °C and 80V, respectively, (6) deposition pressure was 0.3 Pa.

Energy Dispersive Spectrometer (EDS, Oxford, UK) was used to analyze the elementary composition of the Nb–V–N coatings. X-ray diffractometer (XRD, Shimazu-6000, and Japan) was used to investigating microstructure of coatings. Detailed parameters of XRD are following: Cu Kα radiation, operated at 40 kV and 35 mA, scanning speed of 4°/min.A nano-indentation system (CPX + NHT2+MST, Switzerland) was used to measuring hardness of the coating. The detailed paraments are the following: (1) the constant loading force of the first five points were 3 mN, and the final four points were 5 mN. (2) the constant loading force held 10s. A ball-plate wear instrument (UMT-2, USA) using alumina ball counterpart with a diameter of 9.4 mm was used to investigate RT tribology properties of the coatings. The relative humidity was ~55%, the rotation speed was 50 rpm, the load was 3 N and the test duration was 30 min. The elevated temperature (400, 600 and 800 °C) tribological testing was also carried out using the same experimental parameters as the RT ones. Three wear tests were carried on each sample to ensure repeatability of experiments, and use the average value of the long-term steady state in the friction curve as the coating's average *COF*. The tribophases on the wear track surface was evaluated using the X-ray photoelectron spectroscopy (XPS, ESCALAB250XI, Thermo Fisher, USA) to investigate the chemical state of the elements. The experimental parameters could be summarized as follows: (i) the base pressure during the spectra acquisition was below 2×10^{-9} mbr, (ii) Al target operated at 72 W with the hv of 1486.60 eV was chosen as the excitation source and the Au (4f 7/2, 83.96 eV) was chosen as reference to calibrate, (iii) The recorded spectra include valence band and the total acquisition time was 54.2 s, (iv) The spot size of 400 μm was applied during the measurement, (v) Ion beam etching Ar^+ with a primary energy and the angle of 800 eV and 70°, respectively, was carried out for 30 s to remove the surface contaminants, (vi) The fermi level cut-off occurred at 0 eV from the valence band measurements for the sample according to Refs. [14–16]. The deconvolution of spectra was performed using the XPS CASA software, in which an adjustment of the peaks was performed using peak fitting with Gaussian–Lorentzian peak shape and Shirley type background subtraction. The wear rate was obtained by measuring the average cross section area of wear tracks using the 3D Profiler (Dektak-XT, Germany) and combining calculation formula, as follows:

$$W_S = \frac{C \times S}{F \times L}$$

where:

W_S-wear rate($mm^3 \bullet N^{-1} \bullet mm^{-1}$);
C-wear mark perimeter(mm);
S-average area of wear track(mm^2);
F-normal load(N);
L-sliding distance(mm).

3. Results and discussion

Table 1 illustrates the elemental compositions of the Nb–V–N coatings deposited by different V target power. Results confirms that the V content linearly increases with a increase of the V target power, and the corresponding Nb content in the coatings drops gradually. However, the V target power exhibits the slight influence on both the O and N content, with a value remains of ~43 and ~4 at.% respectively. The residual gas in the chamber and absorbed in the wall of the chamber could react with the V or Nb during the deposition and results in the exist of O in the coatings. Besides this, the ratio of V/(Nb + V) also increases gradually with the increase of V target power. The ratio of V/(Nb + V) is defined as V content in the following content of this paper.

Fig. 1 shows the XRD spectra of Nb–V–N coatings with different V contents. As is shown in the figure, there are seven diffraction peaks in the scanning range of the reference NbN coating, which correspond to fcc-NbN (111), hcp-NbN (101), fcc-NbN (200), fcc-NbN (220), single crystal Si substrate, fcc-NbN (311) and fcc-NbN (222) [17–19]. Therefore, the reference NbN coating is composed by fcc-NbN and hcp-NbN [20,21]. Similar phases are detected when V is added at the reference coatings, however, the fcc diffraction peaks shift to higher angles in the direction of the position of the VN phase. This shift is progressive with progressive V concentration, suggesting that V is being incorporated in solid solution in the NbN fcc phase. Similar results were observed for other coatings systems.

TEM was applied to investigate the microstructure of the Nb–V–N coatings, and its image of the cross-sectional coating is shown in Fig. 2. A classic columnar structure of the coating with a V concentration of 12.4 at.% is detected in Fig. 2(a). Its corresponding selected area electron diffraction (SAED) pattern is also presented in Fig. 2(a) as an insert, the result confirms a dual-phase of fcc and hcp NbN co-exists in the coatings, since two kind of diffraction rings appear in the SEAD pattern [22]. Fig. 2(b) illustrates the HRTEM image of the Nb–V–N coating, and the lattice fringe with a spacing of 0.2201 nm is detected. This fringe refers to the fcc-NbN(200). Besides this, obvious dislocations could be observed in the HRTEM due to the solid solution of V into the NbN lattice [23,24].

Fig. 3 shows the hardness and Young's modulus of Nb–N coatings with increasing V content. It can be seen from the figure that with the increase of V content, the hardness of the coating increases firstly and then decreases gradually. When V content is 5.3 at.%, the hardness is the highest, with the highest value of 32 GPa. The change trend of the elastic modulus of the coating is consistent with the hardness, which also reaches the highest value when the V content is 5.3 at.%, and its value is about 410 GPa.

The initial increase of hardness is caused by the solution strengthening of V solid solution in NbN lattice [25–27]. The solid solution of O into the Nb–V–N coatings also induces the solution strengthening, and attributes to the enhancement on the hardness. The further decrease in hardness is explained by the presence of high amounts of bonding

Table 1
Elemental compositions of the Nb–V–N coatings as a function of V target powers.

V target power (W)	Elemental composition (at.%)				
	V/(Nb + V)	Nb	V	N	O
0	0	52.3 ± 2.6	0	43.5 ± 2.2	4.2 ± 0.2
30	5.3 ± 0.2	50.6 ± 2.5	2.8 ± 0.1	42.8 ± 2.2	3.8 ± 0.2
60	12.4 ± 1.0	46.1 ± 2.3	6.5 ± 0.3	43.1 ± 2.2	4.3 ± 0.2
90	17.8 ± 1.0	43.2 ± 2.1	9.4 ± 0.5	43.9 ± 2.2	3.5 ± 0.2
120	25.3 ± 1.0	37.1 ± 1.9	12.6 ± 0.6	45.9 ± 2.2	4.4 ± 0.2

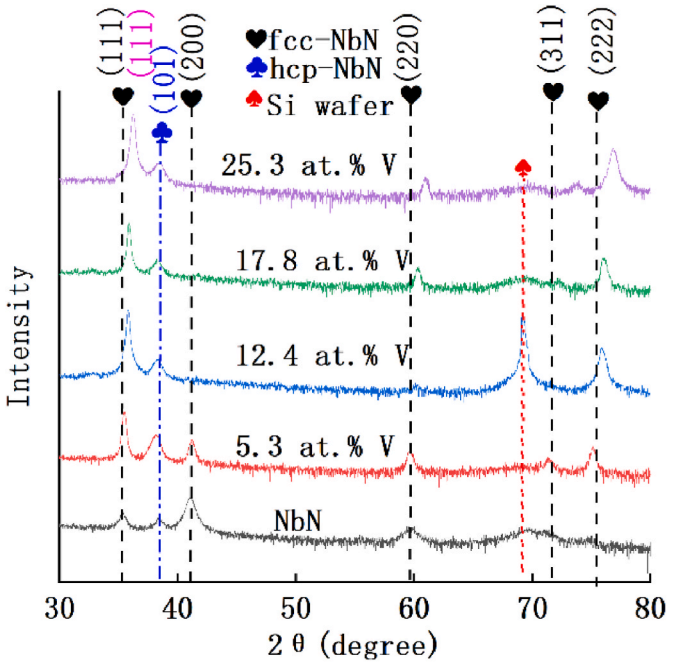

Fig. 1. XRD diffraction patterns of Nb–V–N coatings as a function of V concentrations.

between V–N which are weaker than Nb–N [28,29]. For the elastic modulus, due to the appearance of Nb–V–N replacement solid solution, the lattice constant of NbN is reduced, and the length of each chemical bond is shortened, resulting in the increase of the elastic modulus of Nb–V–N coating with V content of 5.3 at.%. With the further increase of V content, the relative amount of V–N bonds (elastic modulus of 280 GPa) in the coating increases, resulting in the decrease of the overall elastic modulus of the coating.

Fig. 4 shows the average friction coefficient (COF) and wear rate (WR) of Nb–V–N coating with different V content at room temperature. It can be seen from the figure that the COF and WR of binary NbN coating are 0.67 and 2.3 × 10^{-7}mm^3/mmN respectively. The COF and WR of ternary Nb–V–N coating decreased first and then increased with the increase of V content. When the V content was 12.4 at.%, the above two values reached the lowest, with the lowest values of 0.53 and 8.9 × 10^{-8}mm^3/mmN respectively.

In the process of friction, V can react with oxygen and/or water vapor in the environment under the action of friction pairs to generate VO_x friction phase with lubricating effect, which can obviously improve the lubrication performance of the coating [30–32]. Therefore, when the V content in the coating is lower than 12.4 at.%, COF decreases gradually with the increase of V content [33,34]. The existing of O in the as-deposited coatings also attributes to the enhancement on the anti-friction performance, due to the formation of V–O bonds. In addition, at this time, the coating has high hardness and excellent bearing capacity, which can effectively resist the load on the grinding pair, so the WR also gradually decreases with the increase of V content. However, when the V content in the coating is further increased, the hardness of the coating will be greatly reduced, and a large number of V forms wear

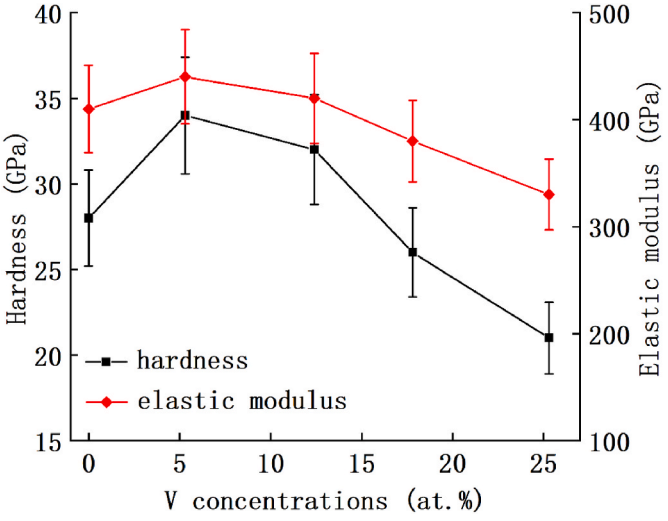

Fig. 3. Hardness and elastic modulus of Nb–V–N coatings as a function of V concentrations.

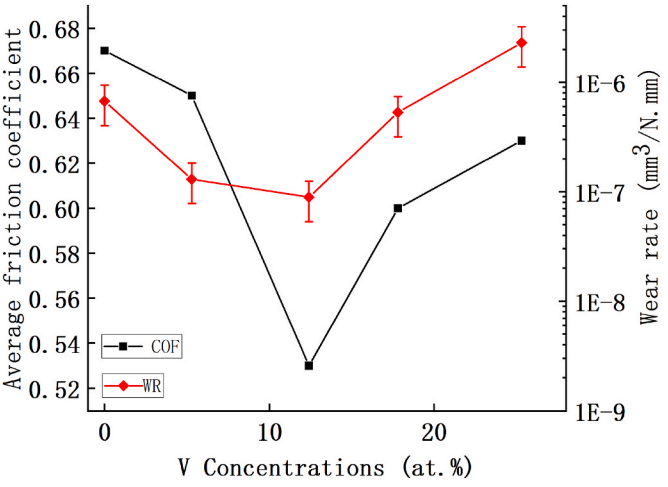

Fig. 4. Average friction coefficient (COF) and wear rate (WR) of the Nb–V–N coatings as a function of V concentrations at room temperature.

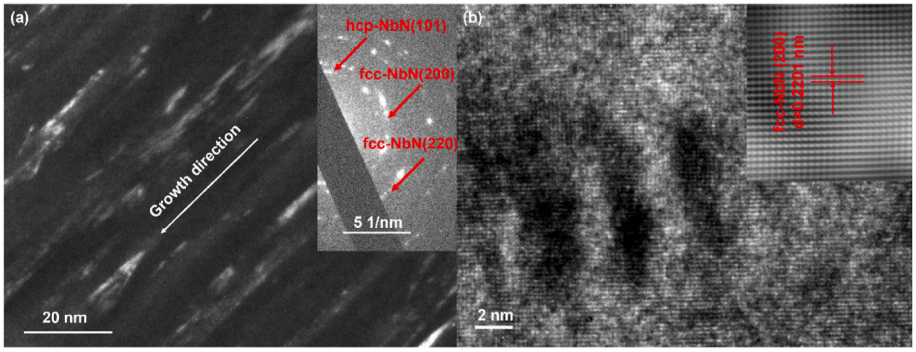

Fig. 2. Cross-sectional TEM image and its corresponding SAED pattern (a), HRTEM and IFFT pattern (b) of the Nb–V–N coating with a V concentration of 12.4 at.%.

debris due to the physical and chemical reaction of friction and adheres to the surface of the wear scar, which hinders the sliding of the wear pair, and finally leads to the gradual increase of COF and WR with the increase of V content [35–37].

Fig. 5 shows the COF and WR of Nb–V–N coating with a V concentration of 12.4 at.% at different testing temperatures. The average friction coefficient of the coating drops gradually from ~0.43 at 400 °C to ~0.30 at 800 °C, whilst the corresponding wear rate increases gradually.

EDS analysis conducted at the wear debris presented on the wear track surface and ball counterpart, revealed that they are mainly V and O rich, with some traces of Nb [38]. This suggests that V–O and Nb–O phases are formed in the contact [39,40]. The V–O tribophase has been widely reported to bean excellent self-lubricant material protecting the coating in the contact during tribological experiments, especially at elevated temperatures [41,42]. Therefore, the formation of V–O phase on the wear track surface during the wear test could enhance the tribological performance of coatings.

Thus, due to the presence of V–O phases in the wear track of coatings, the COF values will be lower than the reference NbN coating. However, the wear debris on the wear track could be easily removed from the contact due to the movement of the ball, resulting in the gradual increase of WR as a function of testing temperatures [44–46].

XPS was applied to investigate the tribophase evaluation at different testing temperatures, and the results is shown in Fig. 6. Nb, V, N and O could be detected in the survey spectra for all sample after the wear test at RT, 400, 600 and 800 °C according to the survey spectra in Fig. 6(a). Besides this, C 1s also appears in this figure, due to the residual gas in the chamber or the adsorbed gas on the sample surface. Four peaks at ~204.1 (Nb–N) [47], ~206.4 (Nb–N) [48], ~207.8 (Nb–O) [49] and ~209.4 eV (Nb–O) [49] appear in the Nb 3d spectra, respectively. Fig. 6 (c) illustrates the V 2p spectrum of the wear track of the film after the RT wear test, and two obvious XPS peaks at ~513 and ~521 eV could be detected in this spectrum, which refers to the V–N bonds [50]. The solution of V into the NbN lattice result in the formation of V–N bonds in the film, and this result is also in agreement with that from the XRD patterns. The XPS spectrum from the wear track of the film after the wear test at 400 °C exhibits there are four XPS peaks: the peaks at ~513 and ~521 eV correspond to the V–N bonds from the as-deposited film, whilst the peak at ~515 eV also appears in the spectrum, referring to the V–O bonds in the V_2O_3 phase [51,52]. Besides this, other peak with a low intensity at ~517 eV is also detected in this spectrum, and this peak could be assigned to the V–O bonds in the V_2O_5 phase [53]. This result confirms that the complex tribochemical reaction under the counterpart, forms the tribophase of V_2O_3 and V_2O_5 during the wear test at 400 °C. But the V_2O_3 could be considered as the dominant one based on its intensity. Four obvious XPS peaks co-exist in the spectrum from the wear track at 600 °C, and the two peaks at ~513 and ~521 eV could be defined as the V–N bonds from the as-deposited phase. The peak at ~515 eV, referring to the V–O bonds in the V_2O_3 phase, is also detected in this figure. Moreover, the intensity of the peak at ~517 eV, corresponding to the V–O bonds in the V_2O_5 phase [53], becomes stronger, compared as the one from 400 °C. This conforms that the tribophase of V_2O_3 gradually transfers to the V_2O_5 phase as the testing temperature increases from 400 °C to 600 °C. As for the spectrum of the wear track at 800 °C, the two XPS peaks corresponding to V–N from as-deposited phase is still detected, whilst the peak at ~515 eV, referring to the V–O bonds in the V_2O_3 phase disappears totally. The peak corresponding to V–O bonds in the V_2O_5 phase could be detected. This suggests the more tribophase of V_2O_3 was transferred to the V_2O_5 during the wear test at 800 °C. Fig. 6(d) illustrates the N 1s spectra of the sample after the wear test at different testing temperatures, and two peaks at ~398.9 and ~402.1 eV could be detected, referring to N–V [54] and N–Nb [55] respectively. The intensity of above two peaks decreases gradually with the increase of the testing temperatures, suggesting that the content of the as-deposited phase of nitride-based phase of NbN decreases, with a corresponding of the increase of oxide based tribophases. As for the O 1s spectra in Fig. 6(e), a single peak at ~530.8 (O–Nb in Nb_2O_3) could be detected for the surface of the wear track at RT. But other two peaks at ~530.0 (O–V in V_2O_5) [51], and ~531.9 eV (O–V in V_2O_3) [51] appear in the spectra of the wear track at 400, 600 and 800 °C.

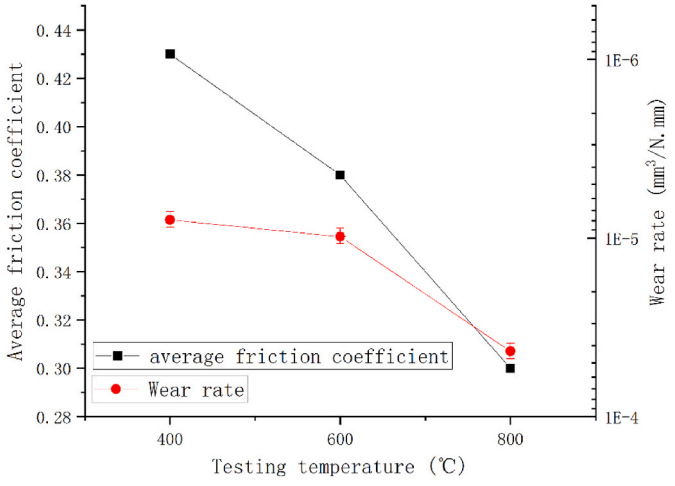

Fig. 5. Average friction coefficient (COF) and wear rate (WR) of the Nb–V–N coating with a V concentration of 12.4 at.% at 400, 600 and 800 °C.

The lubricity of oxide based tribophase could be checked using the principle named crystal chemistry, which was proposed by A. Erdemir for quantitatively evaluating the lubricant capacity of the self-lubricant tribophase using its corresponding ionization potential (Φ). Based on the principle of crystal chemistry, the oxide based tribophase with a higher value of ionic potential usually exhibits a better anti-frictional property. The ionization potential could be calculated by the following formula:

$$\Phi = Z/r$$

Where:

Z—cationvalence
r—cationradius

The value of Z of $V_2O_5$and V_2O_3 is 10.2 and 6.1 respectively, and, hereby the V_2O_5tribophase exhibits a lower friction coefficient during the wear test.

Based on above XPS results, the evaluation of tribophase from the wear track at elevated temperatures from the self-lubricant V_2O_3 at 400 °C to the mix-phase of V_2O_3+V_2O_5 at 600 °C, and finally then totally changing to the V_2O_5 at 800 °C, contributed to the stable and excellent anti-fricitional properties of the coating with a V concentration of 12.4 at.%. However, the wear rate of the coatings drops gradually with the increase of V concentrations due to the large amount of soft but lubricant tribophases at elevated temperatures.

4. Conclusion

A series of Nb–V–N coatings with different V concentrations were deposited using RF magnetron sputtering system, and the influence of V on the crystalline structure, mechanical and tribological properties were investigated. The main conclusion could be summarized as follows:

(1) Adding V into the NbN coating produced a substitutional solid solution where V replaces the positions of Nb in the fcc lattice.
(2) The solid solution strengthening induced by the adding V into the NbN lattice enhanced the hardness of the Nb–V–N coatings from ~28 GPa for NbN coating to ~32 GPa at 5.3 at.% V.
(3) The tribological properties of the coating exhibited a significant dependence on the testing temperatures, which influenced the

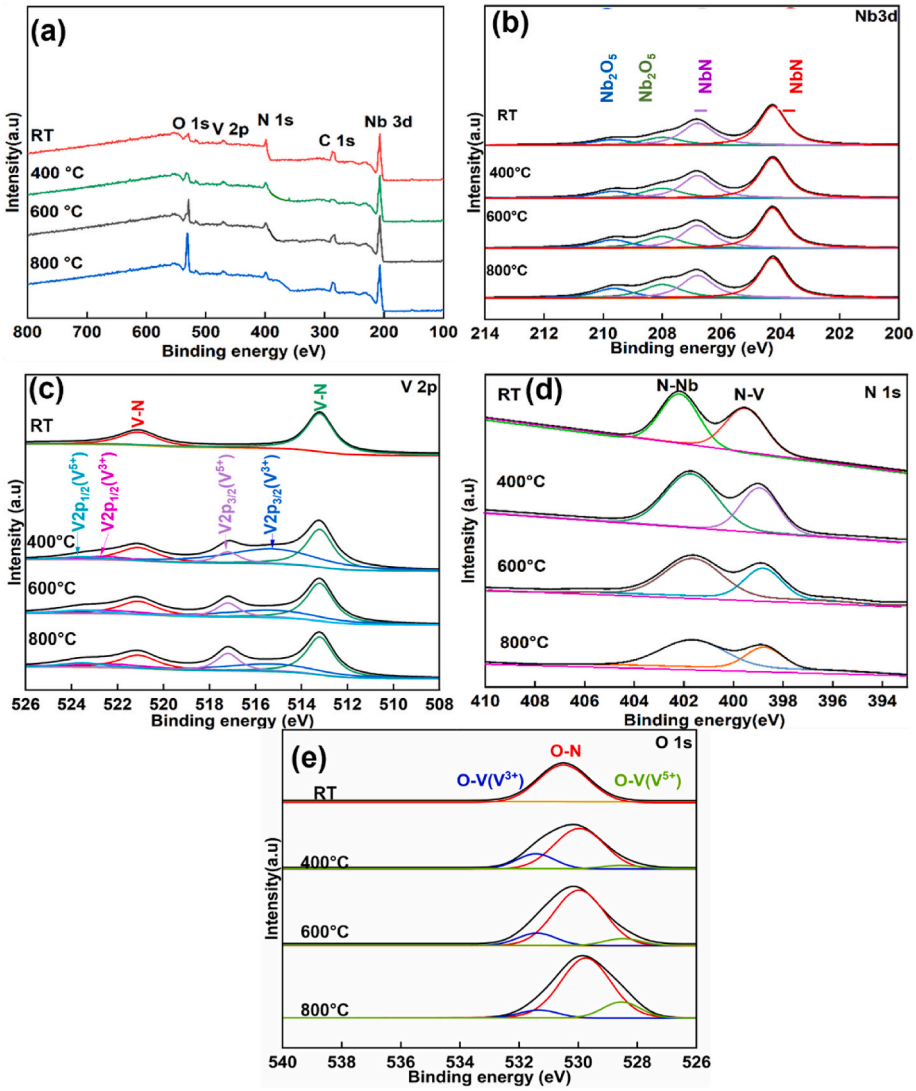

Fig. 6. XPS spectra from the wear track surface of the films after the wear test at different testing temperature of RT, 400 600 and 800 °C: (a) survey spectra, and the high-solution spectra of (b) Nb 3d, (c) V 2p, (d) N 1s, (e) O 1s.

tribophase evaluation on the wear track surface. The evaluation of tribophase from the wear track at elevated temperatures from the self-lubricant V_2O_3 at 400 °C to the mix-phase of V_2O_3+V_2O_5 at 600 °C, and finally then totally changing to the V_2O_5 at 800 °C, contributed to the stable and excellent anti-fricitional properties of the coating with a V concentration of 12.4 at.%. However, the wear rate of the coatings drops gradually with the increase of V concentrations due to the large amount of soft but lubricant tribophases at elevated temperatures.

CRediT authorship contribution statement

Moussa Athmani: Writing – review & editing, Data curation. **Fan-Lin Kong:** Investigation. **Hongbo Ju:** Writing – review & editing, Writing – original draft, Supervision, Resources, Project administration, Methodology, Investigation, Funding acquisition, Formal analysis, Data curation, Conceptualization. **Jing Luan:** Methodology, Data curation, Investigation, Writing – review & editing. **Chengke Zhang:** Writing – original draft, Investigation. **Bingyang Ma:** Investigation, Supervision. **Albano Cavaleiro:** Supervision, Investigation, Funding acquisition, Conceptualization. **Filipe Fernandes:** Resources, Funding acquisition, Conceptualization.

Declaration of competing interest

We declare that we do not have any commercial or associative interest that represents a conflict of interest in connection with the work submitted into VACUUM with a title of "RF magnetron sputtered Nb–V–N self-lubricant composite coatings for high-temperature applications".

Data availability

Data will be made available on request.

Acknowledgement

National Natural Science Foundation of China (51801081, 52171071), Portugal National Funds through FCT scientific contract (2021.04115.CEECIND), as well as the projects of UIDB/00285/2020, LA/0112/2020, MCTool21 project "Manufacturing of cutting tools for the 21st century: from nano-scale material design to numerical process simulation" (POCI-01-0247-FEDER-045940), the European Regional Development Fund, through Portugal 2020 (PT2020), and the Competitiveness and Internationalization Operational Programme (COMPETE 2020). Outstanding University Young Teachers of "Qing Lan

Project" of Jiangsu Province, China, Excellent Talents of “Shenlan Project” of Jiangsu University of Science and Technology, China. The co-first author Fanlin Kong want to his thanks for the supporting from the Post¬graduate Research Innovative Training Program Jiangsu Province, China (SJCX23_2190), Chengke Zhang also thank for the funding from the Undergraduate Innovative Entrepreneurship Training Program of Jiangsu Province, China (202310289056Y).

References

[1] G.S. Fox-Rabinovich, K. Yamamoto, A.I. Kovalev, S.C. Veldhuis, L. Ning, L. S. Shuster, A. Elfizy, Wear behavior of adaptive nano-multilayered TiAlCrN/NbN coatings under dry high performance machining conditions, Surf. Coating. Technol. 202 (2008) 2015–2022.
[2] X. Shang, K. Yu, X. Zuo, H. Yang, Low wear braking material with high friction coefficient, Tribol. Int. 173 (2022), 107608.
[3] H. Ju, P. Jia, J. Xu, L. Yu, Y. Geng, Y. Chen, M. Liu, T. Wei, The effects of adding aluminum on crystal structure, mechanical, oxidation resistance, friction and wear properties of nanocomposite vanadium nitride hard films by reactive magneton sputtering, Mater. Chem. Phys. 215 (2018) 368–375.
[4] P. Zuo, Z. Zhang, X. Qi, Z. Liu, J. Xia, J. Wu, X. Li, B. Zhang, Effects of nanoscale Sn segregation on corrosion behavior of laser powder bed fusion Cu-15Ni-8Sn alloy, J. Mater. Sci. Technol. 158 (2023) 96–110.
[5] A.S. Kuprin, V.D. Ovcharenko, A. Gilewicz, G.N. Tolmachova, I.V. Kolodiy, R. L. Vasilenko, T. Kuznetsova, V. Lapitskaya, B. Warcholinski, Tribol. Int. 165 (2022), 107246.
[6] F. Fernandes, T. Polcar, A. Cavaleiro, Tribological properties of self-lubricating TiSiVN coatings at room temperature, Surf. Coating. Technol. 267 (2015) 8–14.
[7] H. Ju, M. Athmani, J. Luan, A. Al-Rjoub, A. Cavaleiro, T. B. Yaqub, A. Chala, F. Ferreira, F. Fernandes. Insights into the oxidation resistance mechanism and tribological behaviors of multilayered TiSiN/CrVxN hard coatings. Int. J. Miner. Metall. Mater.. https://doi.org/10.1007/s12613-023-2655-0.
[8] H. Ju, J. Xu, Microstructure and tribological properties of NbN-Ag composite films by reactive magneton sputtering, Appl. Surf. Sci. 355 (2015) 878–883.
[9] H. Ju, P. Jia, J. Xu, L. Yu, A. Isaac, Y. Geng, Crystal structure and high temperature tribological behavior of niobium aluminum nitride films, Materialia 3 (2018) 202–211.
[10] D.S. Stone, J. Migas, A. Martini, T. Smith, C. Muratore, A.A. Voevodin, S. M. Aouadi, Adaptive NbN/Ag coatings for high temperature tribological applications, Surf. Coating. Technol. 206 (2012) 4316–4321.
[11] H. Ju, P. Jia, Microstructure, oxidation resistance and mechanical properties of Nb-Y-N films by reactive magnetron sputtering, Protect. Met. Phys. Chem. Surface 562 (2020) 328–332.
[12] P. Eh Hovsepian, D.B. Lewis, Q. Luo, A. Farinotti, Corrosion resistance of CrN/NbN superlattice coatings grown by various physical vapour deposition techniques, Thin Solid Films 488 (2005) 1–8.
[13] H. Ju, N. Ding, J. Xu, L. Yu, Y. Geng, G. Yi, T. Wei, Improvement of tribological properties of niobium nitride films via copper addition, Vacuum 158 (2018) 1–5.
[14] G. Greczynski, L. Hultman, C 1s peak of adventitious carbon aligns to the vacuum level: dire consequences for material’s bonding assignment by photoelectron spectroscopy, Chem. Phys. Chem. 18 (12) (2017) 1507–1512.
[15] G. Greczynski, L. Hultman, The same chemical state of carbon gives rise to two peaks in X-ray photoelectron spectroscopy, Sci. Rep. 11 (2021), 11195.
[16] G. Greczynski, L. Hultman, Compromising science by ignorant instrument calibration—need to revisit half a century of published XPS data, Angew. Chem. Int. Ed. 59 (13) (2020) 5002–5006.
[17] M. Chen, J. Ding, S. Kwon, Q. Wang, S. Zhang, Corrosion resistance and conductivity of NbN-coated 316L stainless steel bipolar plates for proton exchange membrane fuel cells, Corrosion Sci. 196 (2022), 110042.
[18] Y. Ren, X. Liu, X. Tan, S. Sun, H. Wei, F. Lu, Adsorption and pathways of single atomic processes on NbN(001) and (111) surfaces: a first-principle study, Appl. Surf. Sci. 298 (2014) 236–242.
[19] E. Zhang, J. Liu, W. Li, Microstructures, mechanical and tribological properties of NbN/MoS2 nanomultilayered films deposited by reactive magnetron sputtering, Vacuum 160 (2019) 205–209.
[20] V.N. Zhitomirsky, I. Grimberg, L. Rapoport, N.A. Travitzky, R.L. Boxman, S. Goldsmith, A. Raihel, I. Lapsker, B.Z. Weiss, Structure and mechanical properties of vacuum arc-deposited NbN coatings, Thin Solid Films 326 (1998) 134–142.
[21] M. Larsson, M. Bromark, P. Hedenqvist, S. Hogmark, Mechanical and tribological properties of multilayered PVD TiN/NbN coatings, Surf. Coating. Technol. 91 (1997) 43–49.
[22] S.G. Randive, B.J. Lokhande, Spray pyrolyzed hydrophilic nickel oxide electrodes with nano-granular morphology for a symmetric supercapacitor device, J. Alloys Compd. 944 (2023), 169046.
[23] T. Ku, S. Hsu, Y. Lai, S. Chang, S. Tsai, J. Duh, Nano-scale mechanical characteristics of epitaxial stabilization ZrTiN/NbN superlattice coatings, Surf. Coating. Technol. 453 (2023), 129123.
[24] J. Zhang, W. Xin, Z. Ge, G. Luo, J. Peng, Effect of high heat input welding on the microstructures, precipitates and mechanical properties in the simulated coarse grained hear affected zone of a low carbon Nb-V-Ti-N microalloyed steel, Mater. Char. 199 (2023), 112849.
[25] H. Ju, R. Zhou, J. Luan, C.S. Kumar, L. Yu, J. Xu, J. Yang, B. Zhang, F. Fernandes, Tribological performance under different environments of Ti-C-N composite films for marine wear-resistant parts, Int. J. Miner. Metall. Mater. 30 (2023) 144–155.
[26] H. Ju, D. Yu, J. Xu, L. Yu, B. Zuo, Y. Geng, T. Huang, L. Shao, L. Ren, C. Du, H. Zhang, H. Mao, Crystal structure and tribological properties of Zr-Al-Mo-N composite films deposited by magnetron sputtering, Mater. Chem. Phys. 230 (2019) 347–354.
[27] H. Ju, N. Ding, J. Xu, L. Yu, I. Asempah, J. Xu, G. Yi, B. Ma, Crystal structure and the improvement of the mechanical and tribological properties of tungsten nitride films by addition of titanium, Surf. Coating. Technol. 345 (2018) 132–139.
[28] H. Ju, D. Yu, J. Xu, L. Yu, Y. Geng, T. Gao, G. Yi, S. Bian, Microstructure, mechanical and tribological properties of niobium vanadium carbon nitride films, J. Vac. Sci. Technol. A: Vacuum, Surf. Films 36 (3) (2018), 031511.
[29] H. Ju, N. Ding, J. Xu, L. Yu, Y. Geng, F. Ahmed, The tribological behavior of niobium nitride and silver composite films at elevated testing temperatures, Mater. Chem. Phys. 237 (2019), 121840.
[30] N. Fateh, G.A. Fontalvo, G. Gassner, C. Mitterer, Influence of high-temperature oxide formation on the tribological behaviour of TiN and VN coatings, Wear 262 (2007) 1152–1158.
[31] H. Ju, R. Wang, W. Wang, J. Xu, L. Yu, H. Luo, The microstructure and tribological properties of molybdenum and silicon nitride composite films, Surf. Coating. Technol. 401 (2020), 126238.
[32] Z. Zhou, W.M. Rainforth, Q. Luo, P.Eh Hovsepian, J.J. Ojeda, M.E. Romero-Gonzalez, Wear and friction of TiAlN/VN coatings against Al2O3 in air at room and elevated temperatures, Acta Mater. 58 (2010) 2912–2925.
[33] H. Mei, Z. Cai, J. Ding, K. Yan, Q. Li, Z. Zhao, J. Zhao, L. Cheng, M. Liu, W. Gong, The additions of V and Cu on the microstructure and mechanical properties of Mo-N Coatings.Mechanical properties of Mo-N coatings, Coatings 12 (8) (2022) 1129.
[34] C. Liu, H. Ju, J. Xu, L. Yu, Z. Zhao, Y. Geng, Y. Zhao, Influence of copper on the compositions , microstructure and room and elevated temperature tribological properties of the molybdenum nitride film, Surf. Coating. Technol. 395 (2020), 125811.
[35] R. Zhou, H. Ju, S. Liu, Z. Zhao, J. Xu, L. Yu, H. Qian, S. Jia, R. Song, J. Shen, The influences of Ag content on the friction and wear properties of TiCN-Ag films, Vacuum 196 (2022), 110719.
[36] H. Ju, R. Zhou, S. Liu, L. Yu, J. Xu, Y. Geng, Enhancement of the tribological behaviour of self-lubricating nanocomposite Mo2N/Cu films by adding the amorphous SiNx, Surf. Coating. Technol. 423 (2021), 127565.
[37] H. Ju, R. Wang, N. Ding, L. Yu, J. Xu, F. Ahmed, B. Zuo, Y. Geng, Improvement on the oxidation resistance and tribological properties of molybdenum disulfide film by doping nitrogen, Mater. Des. 186 (2020), 108300.
[38] H. Guo, P. Yan, Z. Wu, B. Li, F. Li, J. Hu, Z. Chen, Lubrication mechanisms of Nb-contained oxides characterizing tribochemistry of NiAl/Nb/Ag composites coatings revealed by the density functional theory (DFT) computation, Tribol. Int. 182 (2023), 108352.
[39] H. Ju, S. He, L. Yu, I. Asempah, J. Xu, The improvement of oxidation resistance, mechanical and tribological properties of W2N films by doping silicon, Surf. Coating. Technol. 317 (2017) 158–165.
[40] T. Li, Z. Dong, Y. Zhao, Y. Yuan, Z. Li, H. Lin, S. Han, Reduced Ti-Nb-O nanotube arrays with co-doping of Nb and Ti3+/VO as a high-performance supercapacitor electrode for enhanced electrochemical energy storage, Electrochim. Acta 440 (2023), 141662.
[41] H. Ju, X. He, L. Yu, J. Xu, The microstructure and tribological properties at elevated temperatures of tungsten silicon nitride films, Surf. Coating. Technol. 326 (2017) 255–263.
[42] H. Ju, L. Yu, D. Yu, I. Asempah, J. Xu, Microstructure, mechanical and tribological properties of TiN-Ag films deposited by reactive magnetron sputtering, Vacuum 141 (2017) 82–88.
[44] H. Ju, L. Xu, J. Luan, Y. Geng, J. Xu, L. Yu, J. Yang, F. Fernandes, Enhancement on the hardness and oxidation resistance property of TiN/Ag composite films for high temperature applications by addition of Si, Vacuum 209 (2023), 111752.
[45] H. Ju, R. Zhou, J. Luan, L. Yu, J. Xu, B. Zuo, J. Yang, Y. Geng, L. Zhao, F. Fernandes, Multilayer Mo2N-Ag/SiNx films for demanding applications: morphology, structure and temperature-cycling tribological properties, Mater. Des. 223 (2022), 111128.
[46] G. Greczynski, D. Primetzhofer, J. Lu, L. Hultman, Core-level spectra and binding energies of transition metal nitrides by non-destructive x-ray photoelectron spectroscopy through capping layers, Appl. Surf. Sci. 396 (2017) 347–358.
[47] R. Shu, E.M. Paschalidou, S.G. Rao, B. Bakhit, R. Boyd, M.V. Moro, D. Primetzhofer, G. Greczynski, L. Nyholm, A.l. Febvrier, P. Eklund, Effect of nitrogen content on microstructure and corrosion resistance of sputter-deposited multicomponent (TiNbZrTa)Nx films, Surf. Coating. Technol. 404 (2020), 126485.
[48] Y. Ren, J. Jia, X. Cao, G. Zhang, Q. Ding, Effect of Ag contents on the microstructure and tribological behaviors of NbN–Ag coatings at elevated temperatures, Vacuum 204 (2022), 111330.
[49] G. Greczynski, L. Hultman, Critical method evaluation refutes the Ar 2p signal of implanted Ar for referencing X-ray photoelectron spectra, Appl. Surf. Sci. 635 (2023), 157598.
[50] G. Silversmit, D. Depla, H. Poelman, G.B. Marin, R.D. Gryse, Determination of the V2p XPS binding energies for different vanadium oxidation states (V5+ to V0+), J. Electron. Spectrosc. Relat. Phenom. 135 (2004) 167–175.
[51] H. Chen, C. Liang, S. Xun, Z. Yu, C. Wu, M. He, H. Li, W. i Zhu, Oxygen vacancy regulation strategy in V-Nb mixed oxides catalyst for enhanced aerobic oxidative desulfurization performance, J. Colloid Interface Sci. 641 (2023) 289–298.

[52] B. Podgornik, M. Sedlaček, B. Šetina Batič, M. Čekada, High temperature friction and galling properties of nanolayered (Cr,V)N coatings and effect of V content, Surf. Coating. Technol. 465 (2023), 129594.
[53] A.V. Pshyk, A. Vasylenko, B. Bakhit, L. Hultman, P. Schweizer, T.E.J. Edwards, J. Michler, G. Greczynski, High-entropy transition metal nitride thin films alloyed with Al: microstructure, phase composition and mechanical properties, Mater. Des. 219 (2022), 110798.
[54] E.M. Paschalidou, R. Shu, R. Boyd, At A. Papaderakis, B. Bakhit, A.l. Febvrier, G. Greczynski, P. Eklund, L. Nyholm, The effect of the Nb concentration on the corrosion resistance of nitrogen-containing multicomponent TiZrTaNb-based films in acidic environments, J. Alloys Compd. 927 (2022), 167005.
[55] C. Liu, H. Ju, L. Yu, J. Xu, Y. Geng, W. He, J. Jiao, Tribological properties of Mo2N films at elevated temperature, Coatings 911 (2019) 734.